ELSEVIER

Ceramics International 30 (2004) 597–603

CERAMICS INTERNATIONAL

www.elsevier.com/locate/ceramint

Thermal and mechanical properties of cordierite, mullite and steatite produced by plasma spraying

P. Rohan [a], K. Neufuss [a], J. Matějíček [a,*], J. Dubský [a], L. Prchlík [b,1], C. Holzgartner [b]

[a] *Institute of Plasma Physics, Za Slovankou 3, Praha 18221, Czech Republic*
[b] *Center for Thermal Spray Research, State University of New York, Stony Brook, NY 11794-2275, USA*

Received 20 May 2003; received in revised form 27 May 2003; accepted 1 July 2003

Abstract

Cordierite, mullite and steatite are silicate materials widely used in the ceramics industry. There is, however, only sparse information on their application in plasma spraying and properties of sprayed materials. Plasma sprayed deposits of cordierite, mullite and steatite contain amorphous phases as the result of rapid cooling of molten particles. The amorphous phase has a significant influence on physical properties, especially in connection with heat treatment.

This article deals with phase changes of cordierite, mullite and steatite, resulting from plasma deposition. Special attention is paid to amorphous phase crystallization in subsequent heat treatment.

Plasma sprayed deposits were produced using a water stabilized plasma torch WSP®. The processes taking place in the deposits were examined primarily by differential thermal analysis (DTA), thermal dilatometry (TMA) and X-ray diffraction (XRD). These measurements were complemented by the determination of physical properties (namely, density, Young's modulus and strength) and morphological observations. Important thermal characteristics like crystallization temperature and the coefficient of thermal expansion (CTE) of all materials were determined.

Keywords: B. Porosity; C. Thermal properties; C. Mechanical properties; D. Silicate; Plasma spraying

1. Introduction

Cordierite ceramics, steatite ceramics and mullite are meta-silicates that form the main components of the MgO–Al_2O_3–SiO_2 system. These ceramic materials are widely applied in industry.

Crystalline cordierite is a major component of so-called cordierite ceramics. This type of ceramics consists of the MgO:Al_2O_3:SiO_2 ternary system components in the 2:2:5 ratio. Cordierite ceramics is used mainly in applications requiring high thermal shock resistance, thanks to its very low coefficient of thermal expansion. Cordierite crystallizes in an orthorhombic, pseudohexagonal system, its density is 2.53 g cm^{-3} and melting point 1470 °C. Its mean CTE depends on the cordierite content in the ceramic; typical values are 1.5×10^{-6} to 4.0×10^{-6} C^{-1} in the 25–700 °C temperature range. (For plasma sprayed cordierite, 2.94×10^{-6} C^{-1} is mentioned in [1].)

Mullite ($3Al_2O_3 \cdot 2SiO_2$) is another important ceramic material, featuring good thermal [2] and chemical stability. In the entire temperature range of the crystalline phase, there are no polymorphic transitions that would lead to volumetric changes [3]. It has an orthorhombic crystal lattice, its density is 3.0 g cm^{-3} and melting point 1810 °C.

Steatite ceramics, whose main component is $MgSiO_3$, features high mechanical strength and a low loss factor, and therefore it is widely used in electrical engineering for high frequency applications [4]. In industrial ceramics, it is usually present as an enstatite phase, whose density is 3.21 g cm^{-3}, melting point 1557 °C and crystal lattice is orthorhombic.

Plasma spraying of cordierite, mullite and steatite is only sparsely mentioned in literature and characteristics of the sprayed materials are often inadequate.

Substrate protection by thermally sprayed "substantially pure cordierite to form porous coating" is the subject of a European patent [5]. The amorphous nature of plasma sprayed

* Corresponding author. Fax: +1-420-286586389.
E-mail address: jmatejic@ipp.cas.cz (J. Matějíček).
[1] Present address: Skoda Energo, Tylora 57, 31600 Plzen, Czech Republic.

0272-8842/$30.00
doi:10.1016/j.ceramint.2003.07.004

cordierite was confirmed in [6] by XRD and TEM. Crystallization to μ-cordierite above 830 °C and an irreversible transition a to high-cordierite around 1000 °C was observed [7].

Plasma sprayed mullite is mentioned in a US patent submitted by NASA [8]. Delamination of mullite coating and crack development due to mullite crystallization upon heating of SiO_2 substrate is mentioned.

Thermal barrier coatings (TBC) made from plasma sprayed mullite showed excellent thermal shock resistance up to 1100 °C, but failed above 1200 °C due to phase changes of the SiO_2 phase [2].

Plasma sprayed mullite coatings also exhibited less cracking under thermal cycling than zirconia-based coatings under identical conditions [9]; this was also confirmed in actual diesel engine tests [10].

Plasma sprayed mullite and rare earth silicates as oxygen diffusion barriers under top TBC were investigated in [11]. They succeeded in suppressing the oxidation of the underlying material, but did not show an improvement in thermal cycling performance over zirconia-based coatings due to high temperature degradation.

Earlier work by the authors [12] presented results obtained during studies of plasma sprayed cordierite, wollastonite, mullite and steatite. Plasma sprayed deposits contained an amorphous phase and exhibited less pronounced lamellar structure than usually observed in alumina or zirconia ceramics. Annealing of the deposits for 2 h changed the phase composition and the thermal expansion coefficients. Detailed characteristics of the crystallization of the amorphous materials, such as crystallization temperatures and the extent of shrinkage, were not presented. This fact was the reason for a closer examination of these processes. The measurements were performed on samples from the earlier study, except for wollastonite, whose samples were not preserved.

2. Experimental details

Samples were manufactured using a high-throughput water-stabilized plasma spray system WSP PAL 160 (Institute of Plasma Physics, Prague, Czech Republic). The water in this system is used for stabilizing the electric arc and as a plasma-forming medium. This system operates at about 160 kW arc power and can process large amounts of material per hour.

The materials for this study were pre-processed by milling and sieving to a suitable grain size. Cordierite and steatite powders with grain sizes −90 + 63 μm were prepared by milling electrical components, discarded because of imprecise dimensions. Mullite powder with grain sizes −90 + 63 μm was synthesized at the Institute of Minerals, Kutná Hora, Czech Republic.

The materials were sprayed on steel substrates (plates of size 60 mm × 70 mm × 8 mm). The coatings were about 2.5 mm thick and were stripped from the plates after spraying by a patented process [13] and cut with a diamond saw into smaller pieces as necessary for further tests. The measurements were performed on free-standing deposits, to eliminate the influence of the substrate.

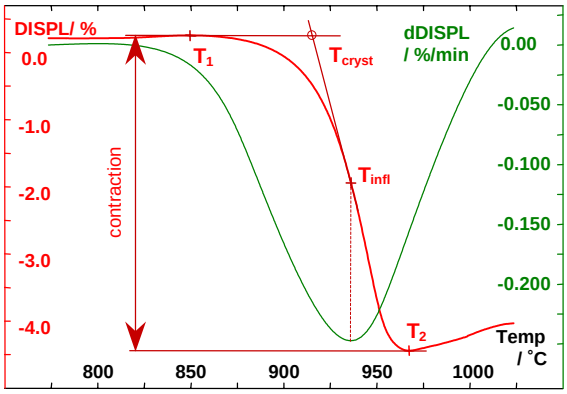

Fig. 1. Denotation of temperatures used in the calculations.

The tests included thermal expansion measurements on samples 12–13 mm long, at a 5 °C min^{-1} rate up to 1350 °C for cordierite, 1480 °C for mullite and 1250 °C for steatite. The measurements were performed on a Setsys 16/18 contact dilatometer (Setaram, France) with a vertical measurement chamber that enables measurements up to 1750 °C in a controlled atmosphere. The thermal expansion coefficients were calculated up to the crystallization and/or transformation temperature for each material.

Denotation of specific temperatures (T_1, T_2, T_{inf}, T_{cryst}) used for the calculation of shrinkage and temperature of crystallization start is shown in Fig. 1.

Powder samples for DTA were obtained by manually grinding the deposits after cutting the dilatometry samples. The sample weight was 90–130 mg, and the measurements were done in Pt containers at a 5 °C min^{-1} heating rate. Due to strong exothermic responses of the processes associated with crystallization, the samples were mixed at a 1:1 ratio with Al_2O_3. The measurements were performed up to 1400 °C.

The crystallization process is usually exhibited on the DTA curve as a strong, sharp peak and on the dilatometric curve as intensive shrinkage on the order of tenths to units of percentage. For all materials studied, full crystallization occurred during the first heating; in subsequent heating cycles, no crystallization response was detected. TMA and DTA measurements enabled us to distinguish processes in the material by their thermal response.

Mullite powder used as a sample for DTA did not sinter or fuse with the Pt cup even upon second heating, in contrast to cordierite and steatite, which were fully compacted after removal. The DTA results were used for selection of maximum temperatures for TMA, to avoid fusing the sample and dilatometry probe.

Density and porosity of the materials was determined by the Archimedean method and He pycnometry [14].

Mechanical properties of the deposits were studied in the as-sprayed state and after heating above the crystallization temperature. In-plane Young's modulus and flexural strength of the free-standing deposits were determined by 4-point bending in an Instron 1362 universal testing machine (Instron, Canton, MA, USA), closely approximating the ASTM C1161 standard [15]. The outer span of the loading fixture was 40 mm and the inner span 20 mm, the specimens were loaded at a crosshead speed of 1 mm min^{-1} and their deflection in the central region was measured by an extensometer. Specimen dimensions were about 2.5 mm × 3.5 mm × 50 mm. Since the materials exhibited a slight non-linearity of the load-deflection curve, two values of Young's modulus will be presented: E_{total}, calculated from the slope of the entire curve up to fracture, and E_{init}, calculated from the initial portion of the curve.

Mechanical anisotropy was studied by an indentation measurement of Young's modulus in two directions (parallel and perpendicular to the spray direction). A Nanotest 600 (Micro Materials Limited, Wrexham Technology Park, LL137YP, UK) depth sensing indentation instrument was used. A 1/32 in. diameter tungsten-carbide ball seated in a brass holder was pressed into polished samples at a constant loading and unloading rate of 80 mN s^{-1}. Continuous measurement of load/displacement records was carried out and the obtained curves were analyzed by the Oliver and Pharr method [16]. Compliance of the machine was determined and corrected for.

Phase composition of the feedstock and the plasma sprayed deposits was examined by X-ray diffraction. A Siemens D500 diffractometer (Siemens, Germany) was used; filtered Co radiation was selected for the majority of the samples.

The morphology of the deposits was studied by scanning electron microscopy SEM (Camscan 4DV, UK).

3. Results

3.1. Structure

The plasma sprayed deposits had an amorphous structure; a lamellar structure, typical for other thermally sprayed deposits, was not observed (see Figs. 2–4).

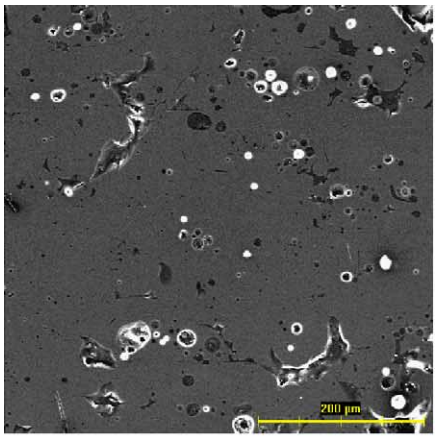

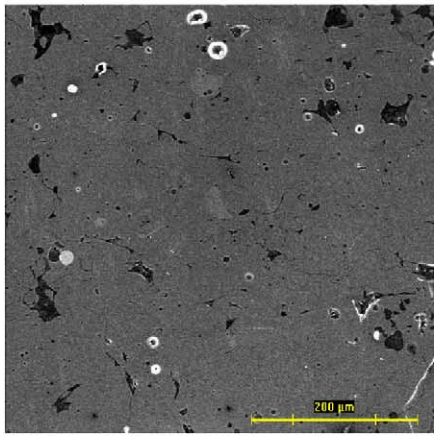

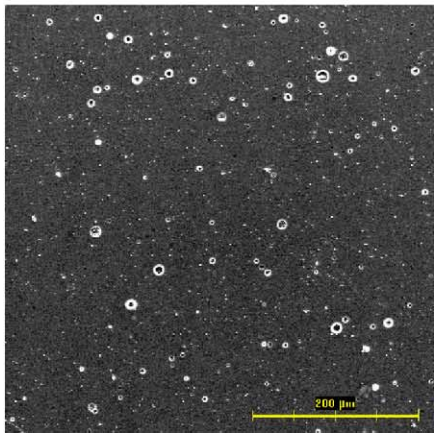

Figs. 2–4. Typical structures of plasma sprayed cordierite, mullite and steatite (cross-sections).

3.2. Thermal properties

3.2.1. Cordierite

The phase composition of the feedstock was cordierite (JCPDS 13-294). Deposits were composed mostly of an amorphous phase with only traces of cordierite. Traces of another crystalline phase were also observed, but could not be identified. Upon heating, the amorphous phase crystallizes to indialite (JCPDS 48-1600). The original crystallographic system of cordierite, i.e., orthorhombic, changed to hexagonal one of indialite.

Thermal processes associated with crystallization of the cordierite glassy phase begin to change the heat flow curve at around 850 °C. The crystallization response is marked by a strong exothermic peak on the DTA curve (Fig. 5). Upon cooling, no such response was observed; thus, the transformation was irreversible. No other thermal processes were found on the DTA curves.

Crystallization of cordierite is exhibited on the dilatation curve by a strong shrinkage (4.7%). The temperatures and

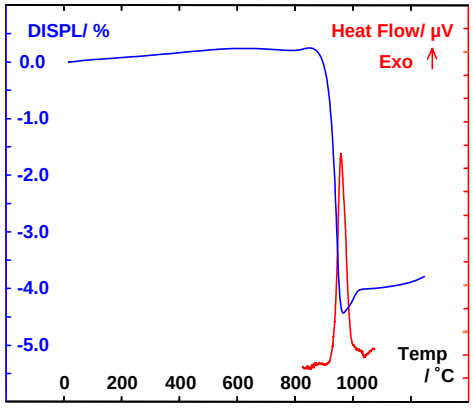

Fig. 5. Thermal expansion and DTA curve of the cordierite deposit at 5 K min^{-1} heating rate.

Table 1
Results of thermal analyses of cordierite, mullite and steatite (denotation of temperatures according to Fig. 1)

	Cordierite	Mullite	Steatite
TMA			
As sprayed CTE 150–620 °C (10^{-6} K^{-1})	3.8	5.2	6.0
Annealed CTE 150–620 °C (10^{-6} K^{-1})	1.3	4.8	8.5
T_1 (°C)	849.6	951.7	804.1
T_{cryst} (°C)	915.3	969.8	855.7
T_{inf} (°C)	936.1	972.8	882.0
T_2 (°C)	967.3	979.0	995.2
Contraction (%)	7.13	0.43	3.25
DTA			
Onset (°C)	937.1	973.3	862.35
Peak top (°C)	958.4	978.0	907.0

shrinkages characterizing the crystallization of each material are summarized in Table 1.

The thermal expansion of the cordierite sample stopped increasing at 650 °C. Between 650 and 790 °C, a slight shrinkage took place. The crystallization itself occurred above 900 °C (see Figs. 5 and 6 and Table 1), and took place fast and in one step.

Mean values of the thermal expansion coefficient were determined in the linear segments of the dilatometric curves

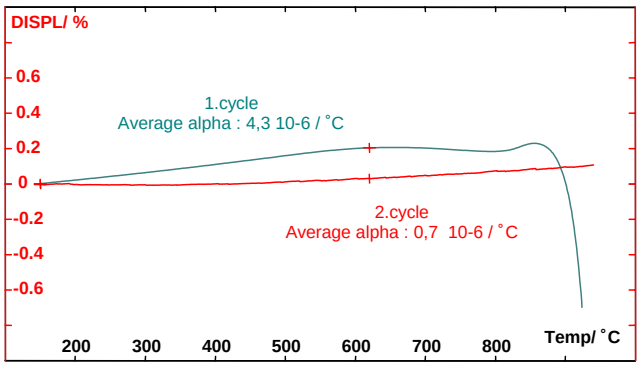

Fig. 6. Thermal expansion of plasma sprayed cordierite.

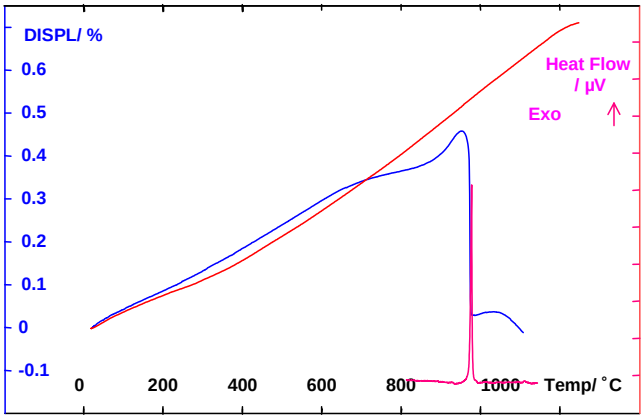

Fig. 7. Thermal expansion of plasma sprayed mullite, during the first and second heating; DTA curve in the crystallization region.

obtained during first and second heating. While the CTE of the as-sprayed cordierite was 3.8×10^{-6} K^{-1}, after crystallization it was 1.3×10^{-6} K^{-1}.

3.2.2. Mullite

Only two phases—mullite and corundum (alpha phase of Al_2O_3)—were observed in the feedstock material. Deposits contained large amounts of amorphous phase and gamma Al_2O_3 phase. Corundum content was reduced below the resolution limit of the XRD. The amount of the mullite phase was also significantly reduced.

The amorphous mullite phase in the deposit crystallized upon heating into mullite again, with the same orthorhombic system.

Upon the first heating of the plasma sprayed sample, crystallization occurred at 970 °C, resulting in about a 0.4% shrinkage (Fig. 7). At the same instant, a regular peak occurred on the DTA curve (Fig. 8). During subsequent heating/cooling cycles, these effects were not observed.

A comparison of the dilatation and heat flow curves at the same heating rate bounds the crystallization of the amorphous mullite to the 970–979 °C temperature interval.

3.2.3. Steatite

The feedstock was composed only of $MgSiO_3$–enstatite (JCPDS 11-273). Deposits were composed only of an

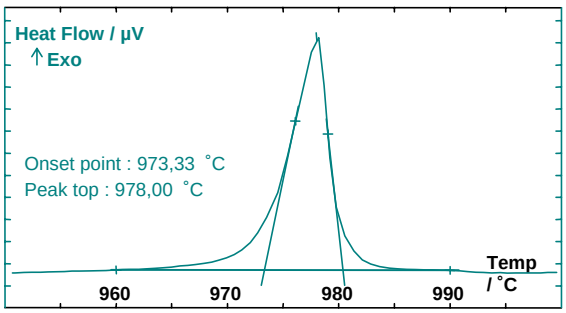

Fig. 8. Crystallization peak during first heating of mullite.

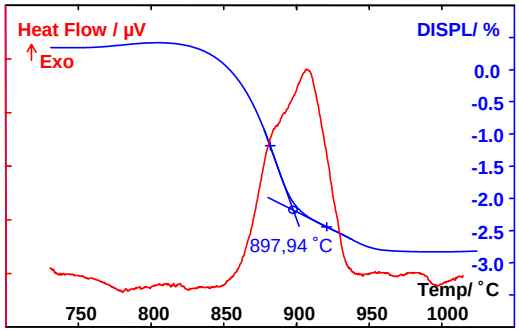

Fig. 9. DTA and TMA curves of steatite deposit in the crystallization region.

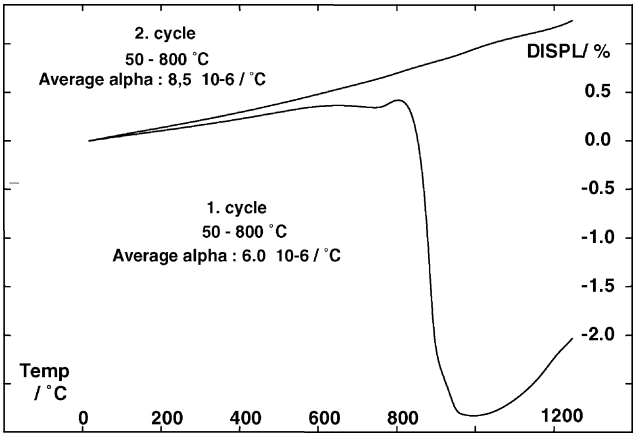

Fig. 10. Thermal expansion curves of plasma sprayed steatite in two subsequent heating cycles.

amorphous phase, with no crystalline peaks being observed.

The phase formed by crystallization of the amorphous deposit is the same as that of the feedstock material, with an identical crystallographic system (orthorhombic).

Non-linearity of the thermal expansion curve occurred about 100 °C before the crystallization itself, as in the other materials studied (cf. Figs. 9–11). While cordierite and mullite crystallized rapidly, steplessly and without any pause, steatite crystallized in two stages, separated by a sharp change of the shrinkage rate on the dilatation curve (at about 900 °C) and the irregular shape of the DTA peak (Fig. 9). This is supposedly a result of the protoenstatite–enstatite transformation.

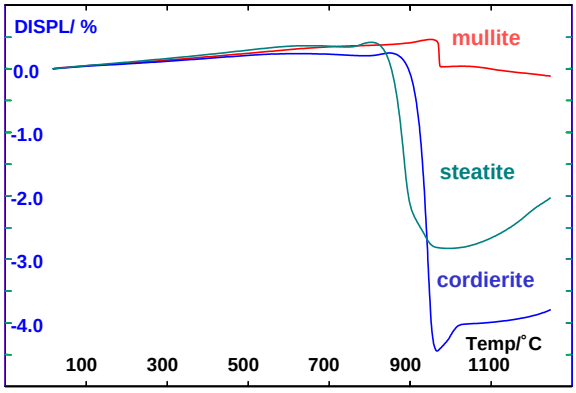

Fig. 11. Thermal expansion curves of cordierite, mullite and steatite during the first heating.

Plasma sprayed steatite, as the only one of the materials tested, exhibited higher CTE after crystallization, $\alpha = 8.5 \times 10^{-6}\,K^{-1}$, than before, $\alpha = 6.0 \times 10^{-6}\,K^{-1}$ (Table 1). During both the first and second heating, the CTE of steatite (as sprayed and annealed) was higher than that of cordierite and mullite. The crystallization shrinkage of steatite, 3.2%, was lower than that of cordierite and higher than that of mullite (Fig. 11). The location of the crystallization response on the DTA agrees with the location of shrinkage on the TMA curve, as was the case with the other two materials studied.

3.2.4. Density

The density and porosity of the feedstock and the deposits are presented in Table 2. The first density value is the skeletal density (i.e., of just the solid), while the apparent density is the density of the entire deposit, including the solid and the pores. Densities of corresponding compact materials, prepared by traditional methods, were presented in Section 1.

3.3. Mechanical properties

Mechanical properties—Young's moduli and flexural strength–of the deposits are summarized in Table 3. Some nonlinearity, indicated by the difference in E_{total} and E_{init}, was noticeable in the steatite deposits, but very small in the mullite and cordierite deposits. A possible reason for this behavior is the gradual opening of microcracks under tensile stress, which reduces the effective material stiffness [17].

Overall, the magnitudes of moduli and strengths are relatively small compared to sintered ceramics, however, the strain tolerance of plasma sprayed deposits is significantly higher (strain to fracture of about 0.001 was observed in all materials). Increased spraying distance resulted in a slightly decreased modulus and strength.

Some anisotropy was observed (by the indentation technique) in the mullite deposits, but not in the cordierite deposits. The values obtained by the indentation technique are generally higher than those obtained by the 4-point bending. This can be again explained by the microcracks present in the deposits; while the loading in indentation is compressive, in the case of 4-point bending it is a mixture of tensile and compressive. The results from both techniques are clearly correlated, describing well the general trends between different materials (Fig. 12). The indentation loading direction used to obtain E_{cross} corresponds to the direction of loading in 4-point bending.

Table 2
Density and porosity of mullite, cordierite and steatite

Material	Density ($g\,cm^{-3}$)	Apparent density ($g\,cm^{-3}$)	Open porosity (%)	Closed porosity (%)
Mullite feedstock	3.073			
Mullite SD 350 mm deposit	2.851	2.648	3.7	7.1
Cordierite feedstock	2.539			
Cordierite SD 350 mm deposit	2.543	2.346	4.5	7.7
Steatite feedstock	2.857			
Steatite SD 350 mm deposit	2.626	2.512	2.5	4.3

Table 3
Mechanical properties of plasma sprayed silicates

Sample	Technique				
	Four-point bending			Indentation	
	E_{total} (GPa)	E_{init} (GPa)	MOR (MPa)	E_{surf} (GPa)	E_{cross} (GPa)
Steatite 350	10 ± 1	17 ± 1	34 ± 2		
Steatite 450	9 ± 1	13 ± 1	28 ± 3		
Cordierite 350	13 ± 1	16 ± 1	40 ± 2	38 ± 9	39 ± 9
Cordierite 450	13 ± 1	16 ± 1	34 ± 1		
Mullite 350	27 ± 2	26 ± 3	91 ± 8	57 ± 5	47 ± 4
Mullite 450	22 ± 3	23 ± 3	75 ± 3		
Cordierite 350 HT	55 ± 3	57 ± 2	51 ± 6	66 ± 6	65 ± 10
Cordierite 450 HT	56 ± 7	60 ± 4	52 ± 8		
Mullite 350 HT	21 ± 2	25 ± 1	29 ± 1	52 ± 5	40 ± 5

The numbers in the first column denote spraying distance in mm. Samples marked 'HT' are heat-treated, all others are as-sprayed. E_{total} is the in-plane Young's modulus calculated from the entire loading period (up to fracture), E_{init} is Young's modulus at the start of loading, and MOR is the modulus of rupture, also called flexural strength. E_{surf} and E_{cross} denote Young's modulus determined from indentation on the deposit surface and cross-section, respectively.

The heat treatment results in a remarkable increase in the modulus of cordierite deposits and a small increase in strength. In the case of mullite deposits, there was a small decrease in the modulus and a greater decrease in strength. The values still fall in a range commonly observed in plasma sprayed ceramics. It can be concluded that these materials retain their structural integrity and thus are usable even after exposure to the crystallization temperature.

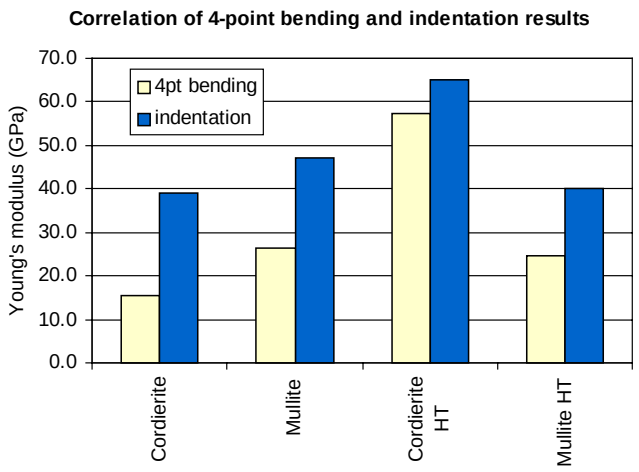

Fig. 12. Correlation of the in-plane Young's modulus obtained by 4-point bending and indentation techniques for as-sprayed and heat-treated cordierite and mullite.

4. Conclusions

Three crystalline ceramic materials—stoichiometric mullite ($3Al_2O_3{\cdot}2SiO_2$), cordierite ($2MgO{\cdot}2Al_2O_3{\cdot}5SiO_2$) and steatite ($MgSiO_3$)—with $-90 + 63\,\mu m$ powder sizes were used for plasma spraying. All three materials studied can be easily sprayed by WSP® to form even millimeters thick deposits.

The deposits exhibited less pronounced lamellar structure than is usually observed in alumina or zirconia ceramics. This can be easily observed especially on the steatite deposits.

As sprayed deposits were totally or mostly composed of an amorphous phase with traces of a crystalline phase. Due to the amorphous phase content, the deposits also had lower thermal expansion coefficient than their bulk counterparts [4] (with the exception of cordierite deposits). The crystalline phase was usually different from the feedstock ($\alpha \rightarrow \gamma Al_2O_3$ in mullite).

Annealing the deposits above 1250 °C changed the phase composition and the thermal expansion coefficient. The phase composition of the annealed deposits was the same as the feedstock phase composition, except for cordierite. While for most of the materials the CTE of the annealed deposit was lower than of the as sprayed one, for steatite the CTE of the annealed deposits increased.

Crystallization of all three plasma sprayed materials exhibited itself by a strong peak on the DTA curve in the 850–980 °C temperature range. This peak did not occur anymore during subsequent heating cycles. It can be assumed that the crystallization behavior will be similar in other meta-silicates, characterized by chain or band structure and commonly used summary formula $M^{II}_2[Si_2O_6]$.

In all three cases, the heat treatment resulted in formation of a stable phase.

In addition to the DTA peak, crystallization was accompanied by a sample length change (Fig. 11). The first heating cycles showed that the largest shrinkage occurred in cordierite (4.7% in the 850–970 °C temperature range). Plasma sprayed mullite showed the smallest amount of shrinkage (0.43% at 950–980 °C) and but the highest temperatures of the crystallization start. Steatite shrunk by 3.2% in the 805–995 °C range.

The sprayed materials have a lower modulus and strength but a higher strain tolerance than similar bulk materials. The magnitudes as well as the anisotropy of the mechanical properties are to some extent affected by the crystallization of the amorphous phase.

Plasma sprayed deposits of cordierite, mullite and steatite with a high content of the glassy phase can find industrial applications. Their use as coatings is limited by the crystallization temperatures of the amorphous phases and associated volumetric changes. Free-standing parts (e.g., tubes or plates), however, undergo crystallization without loss of mechanical integrity.

The experimental results confirm significant differences in the properties of plasma sprayed deposits and materials fabricated by traditional methods. Experimentally determined temperature intervals of crystallization are a prerequisite to developing techniques of production of partially crystalline and amorphous materials by means of plasma spraying.

Acknowledgements

Financial support from the Grant Agency of the Czech Republic under grant no. 106/03/0710 is thankfully acknowledged.

References

[1] H.G. Wang, H. Herman, Thermal-expansion behavior of plasma sprayed cordierite, Mater. Lett. 7 (3) (1988) 69–71.
[2] P. Ramaswamy, S. Seetharamu, K.B.R. Varma, K.J. Rao, Thermal shock characteristics of plasma sprayed mullite coatings, J. Therm. Spray Technol. 7 (4) (1998) 497–504.
[3] H. Schneider, E. Eberhard, Thermal expansion of mullite, J. Am. Ceram. Soc. 73 (7) (1990) 2073–2076.
[4] J. Hlaváč, Základy technologie silikátů SNTL ALFA, Praha, Czech Republic, 1988, (in Czech, Elements of Silicate Technology).
[5] H. Herman, R.W. Iseli, Europatent 0 072 643, February 23, 1983.
[6] H.G. Wang, Y.M. Zhu, H. Herman, Structure of plasma-sprayed oxides in the $MgO–Al_2O_3–SiO_2$ system, J. Mater. Sci. 24 (1989) 4414–4418.
[7] H.G. Wang, G.S. Fischman, H. Herman, Plasma-sprayed cordierite—structure and transformations, J. Mater. Sci. 24 (1989) 811–815.
[8] K.N. Lee, R.A. Miller, N.S. Jacobson, U.S. Patent No. 5 391 404, February 21, 1995.
[9] K. Kokini, Y.R. Takeuchi, B.D. Choules, Surface thermal cracking of thermal barrier coatings owing to stress relaxation: zirconia versus mullite, Surf. Coat Technol. 82 (1/2) (1996) 77–82.
[10] P. Ramaswamy, S. Seetharamu, K. Varma, N. Raman, K.J. Rao, Thermomechanical fatigue characterization of zirconia ($8\%Y_2O_3–ZrO_2$) and mullite thermal barrier coatings on diesel engine components: effect of coatings on engine performance, J. Mech. Eng. Sci. 214 (C5) (2000) 729–742.
[11] Y. He, K.N. Lee, S. Tewari, R.A. Miller, Development of refractory silicate-yttria-stabilized zirconia dual-layer thermal barrier coatings, J. Therm. Spray Technol. 9 (01) (2000) 59–67.
[12] K. Neufuss, J. Ilavský, J. Dubský, B. Kolman, P. Chráska, Plasma spraying of silicates II, in: Proceedings of the United Thermal Spray Conference, Dusseldorf, 1999, pp. 636–640.
[13] K. Neufuss, P. Chráska, Patents (Czech Republic) 283 203, November 25, 1997 and 286 735, April 4, 2000.
[14] K. Neufuss, P. Chráska, B. Kolman, S. Sampath, Z. Trávníček, Properties of plasma-sprayed freestanding ceramic parts, J. Therm. Spray Technol. 6 (4) (1997) 434–438.
[15] ASTM C1161: Standard Test Method for Flexural Strength of Advanced Ceramics at Ambient Temperature, American Society for Testing and Materials, Philadelphia, PA, 1987.
[16] W.C. Oliver, G.M. Pharr, An improved technique for determining hardness and elastic modulus using load and displacement sensing indentation experiments, J. Mater. Res. 7 (6) (1992) 1564–1583.
[17] J. Dubský, J. Matějíček, H.J. Prask, T. Gnaeupel-Herold, Residual and applied stresses in plasma sprayed Cr_2O_3 coatings, Mater. Sci. Forum 404–407 (2002) 419–427.